

Original Article

A naturally derived small molecule NDSM253 inhibits IKK1 to suppress inflammation response and promote bone healing after fracture

Liqi Shen*, Yun Xiao*, Hui Xie, Hongbin Zhao, Tao Luo, Lin Liu, Xuekun Pan

*Department of Emergency Trauma Surgery, The First People's Hospital of Yunnan Province, Kunming, Yunnan, China. *Equal contributors.*

Received July 9, 2020; Accepted December 4, 2020; Epub January 15, 2021; Published January 30, 2021

Abstract: Bone fracture induces an acute inflammatory response in the resident and peripheral monocyte/macrophage cells. Excessive amounts of proinflammatory cytokines can cause severe tissue damage and inhibit bone healing. The proinflammatory cytokine genes are mainly controlled by TLR4/NF- κ B (Toll-like receptor 4/Nuclear factor κ B). Thus, targeting the molecules in this signaling pathway to decrease the expression of proinflammatory cytokines is an effective strategy to inhibit the inflammatory response. Herein, we identified a naturally derived small molecule NDSM253 that specifically inhibited IKK α (Inhibitor of NF- κ B kinase subunit-alpha, a critical component of TLR4/NF- κ B signaling. Biochemically, NDMS253 decreased phosphorylation of I κ B (Inhibitor of NF- κ B), thereby increasing the binding of I κ B-NF- κ B and suppressing the proinflammatory cytokine gene expression. NDMS253 showed a much stronger inhibitory effect on proinflammatory cytokine gene expression than did the known IKK inhibitors, including ACHP (2-Amino-6-[2-(cyclopropylmethoxy)-6-hydroxyphenyl]-4-(4-piperidinyl)-3-pyridinecarbonitrile), IKK16, and Amlexanox. Administration of these IKK inhibitors in a mouse femoral fracture model showed that NDSM253 suppressed proinflammatory cytokine genes, thereby promoting bone healing, while the other three IKK inhibitors showed a weaker improvement of both bone healing and circulating proinflammatory cytokines. Collectively, our data suggested that NDSM253 might be an effective inhibitor of IKK α that could inhibit inflammatory cytokine action in bone injury.

Keywords: NDSM253, IKK1, inflammatory response, proinflammatory cytokine, bone fracture

Introduction

Bone fracture and subsequent repair are two basic issues in orthopedics [1]. Bone healing processes can be divided into four stages: the inflammatory phase, fibrocartilaginous callus formation, bony callus formation, and bone remodeling [2, 3]. These processes involve complicated molecular signaling pathways, so bone injury causes the dysregulated expression of thousands of genes [2, 3]. Once a bone injury occurs, an acute inflammatory response is initiated and the levels of a variety of proinflammatory cytokines, such as IL-1 β (interleukin 1-beta), IL-6, IL-11, IL-15, IL-18, and TNF- α (tumor necrosis factor-alpha), significantly increase during this process [2, 3]. The accumulation of these proinflammatory cytokines attracts immune cells (i.e., macrophages and

monocytes) to the fractured sites to remove damaged tissues and secrete VEGF (vascular endothelial growth factor) [2, 3]. The secretion of VEGF triggers angiogenesis, thereby contributing to the formation of fibrin-rich granulation tissues [2, 3]. Meanwhile, mesenchymal stem cells (MSCs) in the fracture sites promote callus formation by differentiating into fibroblasts, chondroblasts, and osteoblasts [4, 5]. Osteoblasts express several proinflammatory cytokines, including IL-1 β , IL-6, IL-11, IL-12, TNF- α , and IFN- γ (interferon- γ), which promote bone remodeling [6, 7]. The important roles of proinflammatory cytokines in the inflammatory versus the bone remodeling phases suggest that therapies that target the signaling pathways involved in regulating proinflammatory cytokines may improve the outcome of patients with fractures [2, 3, 6, 7].

NDSM253 promotes bone healing

The expression of proinflammatory cytokine genes has been studied extensively. Overall, these genes are mainly controlled by a variety of transcription factors, such as NF- κ B (Nuclear factor κ B), AP1 (Activator protein 1), and STATs (Signal transducer and activator of transcription) [8, 9]. Of these factors, the TLR4 (Toll-like receptor 4)/NF- κ B signaling pathway plays a central role in the regulation of proinflammatory cytokine genes [8, 9]. Harmful stimulators, such as lipopolysaccharide (LPS) and HMGB1 (high-mobility group box protein 1), can bind to the TLR4 membrane receptor, which then recruits its intracellular adaptor proteins, including MyD88 (Myeloid differentiation primary response gene 88), TIRAP (TIR domain-containing adaptor protein), BTK (Bruton tyrosine kinase), TRAM1 (Translocation associated membrane protein 1), and TRIF (TIR-domain-containing adapter-inducing interferon- β) [8-10]. The activation of TLR4 and its intracellular adaptor complex triggers TRAF6 (TNF receptor-associated factor 6), causing the induction of TRAF6 downstream molecules that include TAK1 (Transforming growth factor- β -activated kinase 1) and IKKs (Inhibitor of NF- κ B kinase) [8-10]. The IKKs phosphorylates the inhibitor of NF- κ B (I κ B) and phosphorylated I κ B dissociates from the NF- κ B complex [8-10]. The disassociated-I κ B is recognized and degraded by a specific E3 ubiquitin ligase SCF (β -TrCP) that releases NF- κ B subunits, which then translocate from the cytoplasm to the nucleus to initiate the transcription of proinflammatory cytokine genes [8-10].

A critical step in the activation of NF- κ B is the phosphorylation of I κ B mediated by IKKs, which is composed of three subunits: IKK α (IKK1), - β (IKK2), and - γ (I κ BKG) [11, 12]. Among these three subunits, IKK α and IKK β are catalytically active, whereas IKK γ has a regulatory function [11, 12]. In the past decades, a great number of IKK inhibitors have been shown to attenuate the inflammatory response by blocking the phosphorylation of I κ B [13, 14]. These IKK inhibitors can be grouped into three classes: ATP-dependent compounds that interact with IKKs, compounds that allosterically affect IKK structure, and compounds that interact with a specific cysteine (e.g., Cys-179) residue of IKK β [13-15]. Some of these reported IKK inhibitors are commercially available. For instance, 2-amino-

6-[2-(cyclopropylmethoxy)-6-hydroxyphenyl]-4-(4-piperidinyl)-3-pyridinecarbonitrile (ACHP) is a selective inhibitor that targets both IKK α and IKK β with low IC₅₀ values (250 nM for IKK α and 8.5 nM for IKK β) [14]. BI605906 is a selective IKK β inhibitor with an IC₅₀ value of 380 nM [16]. BMS345541 is a selective allosteric inhibitor of both IKK α and IKK β , with IC₅₀ values of 0.3 and 4 mM, respectively [17]. IKK16 is a selective allosteric inhibitor of both IKK α and IKK β , with IC₅₀ values of 200 and 40 nM, respectively [18]. TPCA1 is a selective IKK β inhibitor with an IC₅₀ value of 17.9 nM [19]. Although many compounds have been reported to inhibit IKKs, few of them can specifically target IKK α [13-15] but instead effectively inhibit IKK β [13-15]. This has necessitated the screening for specific inhibitors of IKK α to explore the effects of IKK α blockage on the expression of proinflammatory cytokines and the inflammatory response.

In this study, we established a mouse femoral fracture model and revealed activation of the TLR4/NF- κ B axis and significant induction of proinflammatory cytokines. We obtained small molecules that specifically inhibited IKK α by establishing a fluorescent-linked enzyme chemoproteomic strategy (FLECS) and screening IKK α inhibitors in a naturally derived small molecule (NDSM) pool. We obtained a small molecule, named NDSM253, which showed inhibitory IC₅₀ values of 13.5 nM, 745.6 nM, and 81.6 mM against IKK α , IKK β , and IKK γ , respectively. The promising inhibitory effect of NDSM253 on IKK α encouraged us to conduct further investigations on its suppressive effect on proinflammatory cytokine gene expression and to evaluate its role in bone healing *in vivo*.

Materials and methods

Establishment of mouse femoral fracture model

Femoral fractures were generated in mice following a previously described protocol [20]. In brief, 10-week-old C57BL/6J mice (The Jackson Laboratory, Bar Harbor, ME, USA) with similar weight (~30 g) were anesthetized by intraperitoneal injection of a mixture of ketamine (100 mg/kg) (Sigma-Aldrich, Shanghai, China, #K2753) and xylazine (10 mg/kg) (Sigma-Aldrich, #X1251). The mice were fixed in

NDSM253 promotes bone healing

place and the femoral bones were hit with a 400 g weight from 40 cm above. The fractured mice were then divided into a non-stabilization and a stabilization group. The non-stabilization group mice were allowed to recover individually in cages after fracture. The stabilization group mice had the fractured femoral bone sites wiped down with 70% ethanol and the fur removed. A preoperative dose of buprenorphine hydrochloride analgesia (0.05 mg/kg; Sigma-Aldrich, #PHR1729) was administered subcutaneously and a 2 cm incision was made using a scalpel blade. The fractured femoral bones were stabilized with 4 cm long stainless steel (Wuhan Third Medical Device Factory, Wuhan, China) and the incision site was closed with an absorbable suture (Sigma-Aldrich, #719846). The surgically treated mice were allowed to recover individually in cages. After a three-day recovery period, serum and the tissues around the fractured bone were collected. All these mouse experiments were performed following a protocol approved by the Institutional Animal Care and Use Committee (IACUC) of the First People's Hospital of Yunnan Province.

Enzyme-linked immunosorbent assay (ELISA)

The serum concentrations of cytokines were measured by ELISA following a previous method [21]. Briefly, the collected blood samples were centrifuged at 1000 g for 10 min. ELISA kits were used to measure cytokine concentrations, including IL-1 β (Sigma-Aldrich, #RAB0274), IL-4 (Sigma-Aldrich, #RAB0300), IL-6 (Sigma-Aldrich, #RAB0308), IL-13 (Sigma-Aldrich, #RAB0257), IL-15 (Sigma-Aldrich, #RAB0260), IL-18 (Sigma-Aldrich, #RAB0810), and TNF- α (Sigma-Aldrich, #RAB0477), in the supernatants.

Cell lines and transfection

Two bone marrow macrophage-derived osteoclast cell lines, LADMAC (#CRL-2420) and 23ScCr (CRL-2751), were purchased from the American Type Culture Collection (ATCC, Manassas, VA, USA). Cells were grown in Dulbecco's Modified Eagle Medium (DMEM) (Sigma-Aldrich, #D5796) supplemented with 10% fetal bovine serum (FBS) (Thermo Fisher Scientific, Shanghai, China, #26140079), and 100 U/mL penicillin-streptomycin (Thermo Fisher Scientific, #15140122). Cells were incu-

bated at 37°C and 5% CO₂, with medium renewal every three days. The pCDNA3-EGFP-IKK1 plasmid was transfected into LADMAC cells using a HiPerFect Transfection Reagent (QIAGEN, USA, #301704) according to the manufacturer's protocol.

Screening IKK α inhibitors by FLECS

The IKK α inhibitors were identified using the FLECS method, as described previously [22]. In brief, cells expressing pCDNA3-EGFP-IKK1 were lysed in cell lysis buffer (150 mM NaCl, 50 mM Tris pH 7.5, 1% Triton X-100, 1 mM EDTA, 1 mM DTT, and 1 \times protease inhibitor cocktail). After centrifuging at 13,000 rpm for 15 min, the supernatant was combined with P-linked ATP Sepharose, which was prepared following a previous protocol [22]. The column was rinsed with 10 column volumes of high-stringency wash buffer (500 mM NaCl, 25 mM Tris pH 7.5, 60 mM MgCl₂, and 1 mM DTT), and 10 column volumes of low-stringency wash buffer (100 mM NaCl, 25 mM Tris pH 7.5, 60 mM MgCl₂, and 1 mM DTT). Equal volumes (50 mL) of a mixture of resin and low-stringency wash buffer (1:1, v/v) were distributed into 96-well plates and the small molecule inhibitors (1 μ M) were added and incubated at room temperature for 10 min in the dark. The plates were centrifuged to clarify the solutions and read in a microplate reader (Promega, Madison, WI, USA, #GM3000) to determine the fluorescence intensity in each well.

Cell treatment

Cells under 80% confluence were treated with 14 nM NDSM253, 10 nM ACHP (Bio-Techne, Minneapolis, MN, USA, #4547), 55 nM IKK16 (Bio-Techne, #2539), 22 nM TPCA (Bio-Techne, #2559), or 2.5 mM Amlexanox (Bio-Techne, #4857) for 6 h. Cells were then washed twice with PBS, and subjected to RNA and protein isolation.

Western blotting

Total cell extracts were isolated with RIPA buffer (Sigma-Aldrich, #R0278) containing 1 \times protease inhibitor cocktail, and centrifuged at 13,000 rpm for 15 min. The cytoplasmic and nuclear fractions were isolated with the NE-PER™ Nuclear and Cytoplasmic Extraction

NDSM253 promotes bone healing

Kit (Thermo Fisher Scientific, #78833), according to the manufacturer's protocol. The total extracts and the cytoplasmic and nuclear proteins were quantified using a Nanodrop spectrophotometer (Thermo Fisher Scientific, #9836674). Equal amounts of protein were loaded onto 10% SDS-PAGE gels. The western blotting procedures and antibodies (anti-TLR4, anti-MyD88, anti-TRAF6, anti-p65, anti-p50, anti-LSD1, anti- β -actin and anti-GAPDH) were as described previously [21]. Additional antibodies included: anti-TIRAP (Abcam, Shanghai, China, #ab17218), anti-TAK1 (Abcam, #ab50431), anti-IKK1 (Abcam, #ab227852), anti-plkB (Abcam, #ab109509), and anti-IkB (Abcam, #ab133462).

Total RNA extraction and real-time quantitative PCR (RT-qPCR) analysis

Total RNA was extracted from cells and tissues using TRIzol reagent (Thermo Fisher Scientific, #15596026) and quantified with a Nanodrop spectrophotometer. A 1 mg sample of total RNA was used to synthesize cDNA with a High-Capacity cDNA Reverse Transcription Kit (Thermo Fisher Scientific, #4368813). The obtained cDNA was applied to RT-qPCR analyses to detect gene expression with the following primers: mL-1 β Forward: TCAGCACCTCACAAGCAGAGCAC, mL-1 β Reverse: GAAGGCATTAGAAACAGTCCAG; mL-6 Forward: AGTCACTTTGAGATCTACTCGGC, mL-6 Reverse: CATATTGTCAGTTCTTCGTAGA; mL-15 Forward: ATAGCCAGCTCATCTTCAACATTG, mL-15 Reverse: ATGAAGACATGAATGCCAGCCT; mL-18 Forward: AGTAAGAGGACTGGCTGTGAC, mL-18 Reverse: TTGTTGTGCTCTGGAACACGT; mTNFA Forward: ATATACCTGGGAGGAGTCTTCCA, mTNFA Reverse: ACACCCATTCCCTTCACAGA; mICAM1 Forward: CAAGAAACGCTGACTTCATTCTC, mICAM1 Reverse: AAGAAGAGTTGGGACAATGT; mL-4 Forward: ATCACTTGAGAGAGATCATC, mL-4 Reverse: TCACTCTCTGTGTGTTCTT; mL-13 Forward: AATGAGTCTGTCAGTATCCC, mL-13 Reverse: TACAGTGAGGTAGCAGAGT.

Scoring system for fracture healing

The scoring system used for fracture healing followed a previous standard [23]. Two major categories, callus formation and bone union, were scored with the following standards: for callus formation, 5 (full-across the fracture), 4 (high, >70% across), 3 (moderate, 50-70%

across), 2 (moderate/mild, 25-50% across), 1 (mild, <25% across), and 0 (no callus); for bone union, 1 (mild, <50%), 2 (moderate, >50%), and 3 (full across the defect). For bone union, 5 (full bone bridge union), 4 (high, >70% bridge), 3 (moderate, 50-70% bridge), 2 (moderate/mild, 25-50% bridge), 1 (mild, <25% bridge), and 0 (no bridge).

Statistical analysis

All experiments were independently repeated at least three times. Data were presented as the mean \pm standard deviation (SD). The statistical significance was determined using a two-sided Student's *t* test and one-way analysis of variance (ANOVA). $P < 0.05$ (*), $P < 0.01$ (**), and $P < 0.001$ (***)).

Results

Bone fracture in mice caused a significant induction of proinflammatory cytokines

We used a mouse femoral fracture model to investigate the molecular changes occurring after bone fracture. The fractured bones were stabilized with or without stainless steel rods (**Figure 1A** and **1B**). After three days of fracture, we measured the serum concentrations of five proinflammatory cytokines, including IL-1 β (**Figure 1C**), IL-6 (**Figure 1D**), IL-15 (**Figure 1E**), IL-18 (**Figure 1F**), and TNF- α (**Figure 1G**). The ELISA results showed that these five proinflammatory cytokines were significantly induced in both the non-stabilization and stabilization groups when compared to a sham group (**Figure 1C-G**). Comparison of their concentrations in the non-stabilization and stabilization groups revealed that surgical stabilization could further induce the production of these five proinflammatory cytokines (**Figure 1C-G**). We also measured the levels of IL-4 and IL-13. The ELISA results indicated that the concentrations of these two proinflammatory cytokines did not differ significantly in the sham, non-stabilization and stabilization groups (**Figure 1H** and **1I**). These results suggested that an acute inflammation response was a common phenomenon in the early stage of bone fracture.

Bone fracture in mice activated the TLR4/NF- κ B signaling pathway

The proinflammatory cytokine genes are mainly regulated by the TLR4/NF- κ B signaling

NDSM253 promotes bone healing

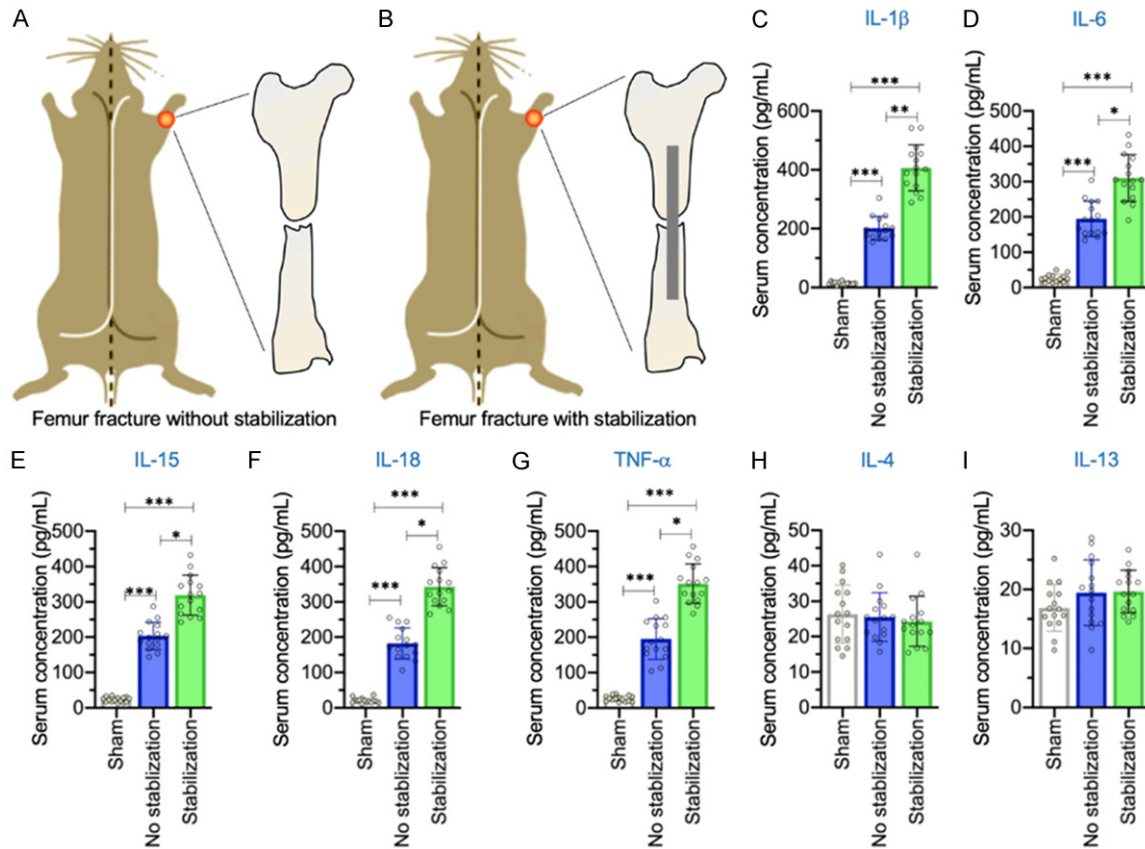


Figure 1. Serum concentrations of proinflammatory cytokines were increased in mouse femoral fracture models. (A and B) Schematic diagrams of mouse femoral fracture models. (A) non-stabilization; (B) stabilization. (C-I) Serum concentrations of cytokines. Circulating levels of IL-1 β (C), IL-6 (D), IL-15 (E), IL-18 (F), TNF- α (G), IL-4 (H), and IL-13 (I) were measured in serum samples obtained from sham, non-stabilization, and stabilization group mice (n=10 for each group). * P <0.05, ** P <0.01, and *** P <0.001.

pathway, and we found a significant induction of proinflammatory cytokines in the mouse fracture model (Figure 1), implying activation of the TLR4/NF- κ B signaling pathway in this pathological process. This possibility was confirmed by the detection of protein levels of several critical molecules, including TLR4, TIRAP, MyD88, TRAF6, TAK1, IKK1, pI κ B, I κ B, p65 and p50, in three representative samples of the sham, non-stabilization and stabilization groups. The immunoblot results indicated a significant induction of TLR4, TIRAP, MyD88, TRAF6, TAK1, IKK1, and pI κ B in both the non-stabilization and stabilization groups compared to the sham mice (Figure 2A and 2C). A comparison of the differences between the non-stabilization and stabilization groups revealed a much greater abundance of these proteins in the stabilization group than in the non-stabilization group (Figure 2A and 2C). By

contrast, the protein level for I κ B was higher in the sham and the non-stabilization group than in the stabilization group (Figure 2A and 2C). However, the p65 and p50 protein levels did not show significant differences (Figure 2B and 2D).

The translocation of NF- κ B from the cytoplasm to the nucleus is necessary for transcription of proinflammatory cytokine genes [10]. Isolation of the cytoplasmic and nuclear fractions revealed a significant decrease in the cytoplasmic fractions of p65 and p50 and a significant increase in their nuclear fractions in the stabilization and non-stabilization groups compared to the sham group mice (Figure 2B and 2D). A similar significant change was also observed for p65 and p50 in the stabilization group compared to the non-stabilization group (Figure 2B and 2D). These results supported an

NDSM253 promotes bone healing

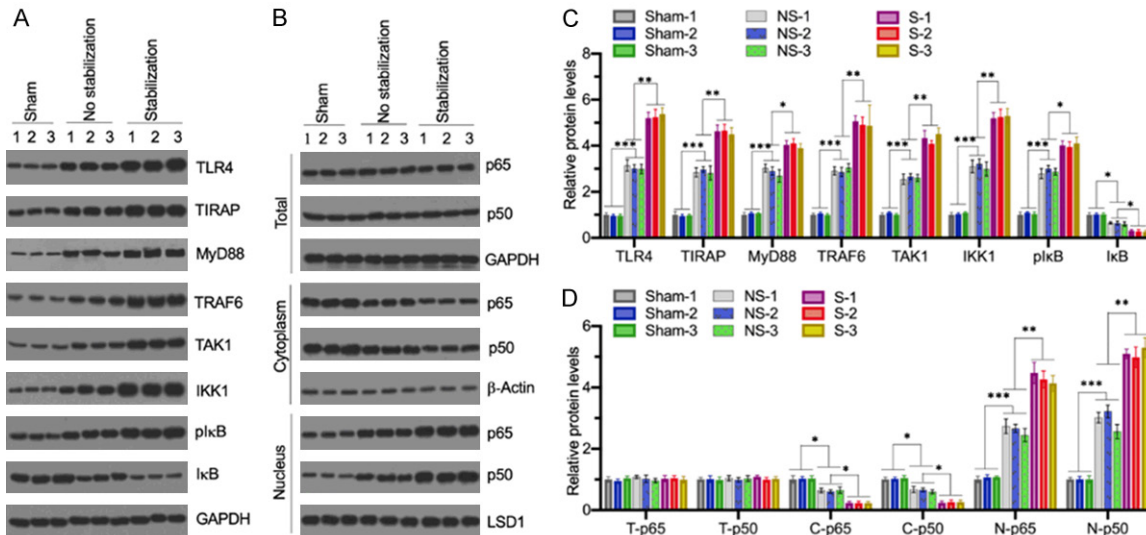


Figure 2. The TLR4/NF- κ B signaling pathway was activated in mouse femoral fracture models. (A) The protein levels of TLR4/NF- κ B molecules. The protein levels of TLR4, TIRAP, MyD88, TRAF6, TAK1, IKK1, pI κ B, and I κ B were determined by western blotting analyses. GAPDH was used as the loading control in the total cell extracts. (B) The protein levels of p65 and p50. The total, cytoplasmic, and nuclear levels of p65 and p50 proteins were determined by western blotting analyses. β -actin was used as a cytoplasmic loading control and LSD1 was used as a nuclear loading control. (C and D) The quantified protein levels. The protein bands in (A) and (B) were quantified using Image J software and then normalized to their corresponding loading controls. (C) The quantified protein levels of (A). (D) The quantified protein levels of (B). * $P < 0.05$, ** $P < 0.01$, and *** $P < 0.001$.

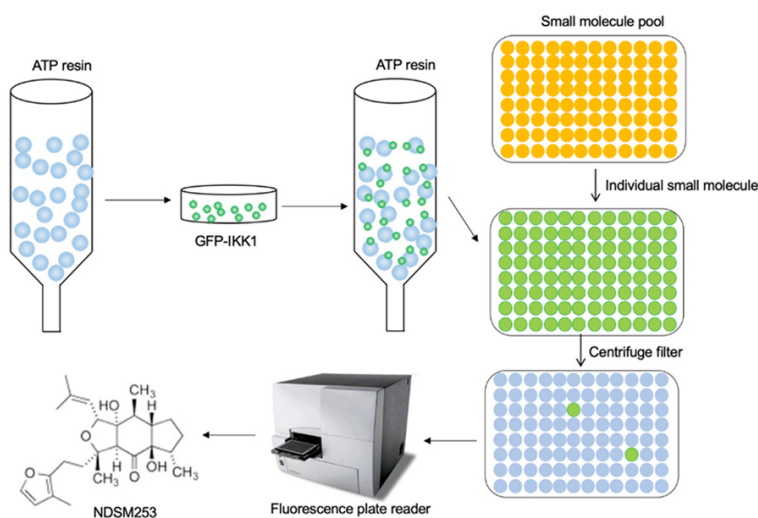


Figure 3. The schematic diagram of screening NDSM253 by FLECS. Total protein extracts were prepared from cells expressing pCDNA3-EGFP-IKK1 and flowed through an ATP resin column. The column was washed with high salt and low salt solutions and the ATP resin-bound proteins were distributed into 96-well plates and a small molecule was added to each well. After centrifuging to filter, the eluted proteins were subjected to measure fluorescence in a fluorescence plate reader. Small molecules that caused fluorescence intensities > 3000 were selected as potential candidates. The chemical structure of NDSM253 is shown.

NDSM253 specifically inhibited IKK1 activity in vitro

The activation of IKKs is critical for the induction of proinflammatory cytokines [10]; therefore, we also screened small molecules using IKK1 as a target. We transfected pCDNA3-EGFP-IKK1 into LADMAC cells and then incubated cell lysates with ATP resin to bind GFP-IKK1. The mixture was equally distributed into 96-well plates and individual small molecules (a total of 1233 small molecules) were added into each well (Figure 3). Small molecules that caused fluorescence intensities > 3000 were selected as potential candidates. The FLECS results indicated that a small molecule NDSM253 could significantly

decrease IKK1 activity; its chemical structure was shown in Figure 3.

decrease IKK1 activity; its chemical structure was shown in Figure 3.

NDSM253 promotes bone healing

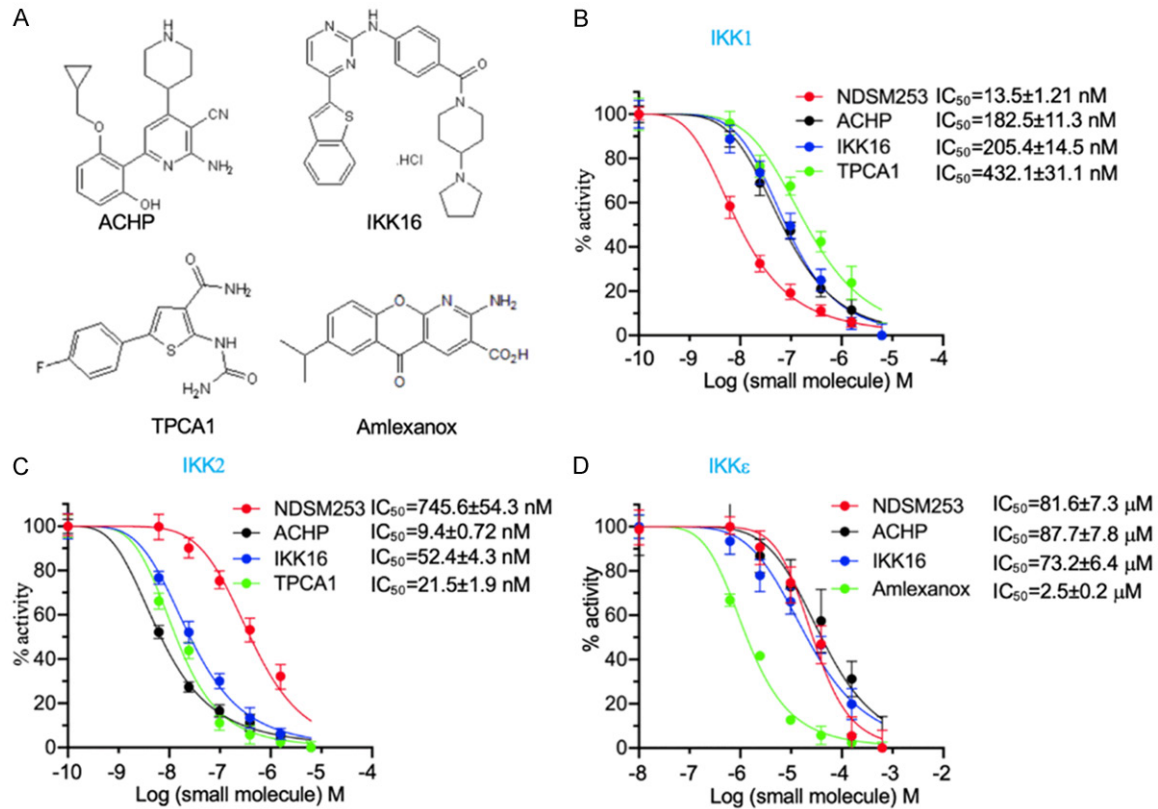


Figure 4. The determination of the inhibitory effect of NDSM253 on IKK proteins. A. The chemical structure of ACHP, IKK16, TPCA1 and Amlexanox. B. The inhibitory effects of IKK inhibitors on IKK1. The purified His-IKK1 protein and different concentrations of IKK inhibitors were used in luminescent kinase assays to determine IC₅₀ values of the IKK inhibitors. C. The inhibitory effects of the IKK inhibitors on IKK2. The purified His-IKK2 protein and different concentrations of IKK inhibitors were subjected to luminescent kinase assays to determine IC₅₀s of IKK inhibitors. D. The inhibitory effects of IKK inhibitors on IKKε. The purified His-IKKε protein and different concentrations of IKK inhibitors were subjected to luminescent kinase assays to determine IC₅₀ values of IKK inhibitors.

We determined the inhibitory efficiency and specificity of NDSM253 by purifying his-IKK1, his-IKK2, and his-IKKγ and performing a luminescent kinase assay. We also used several known IKK inhibitors (ACHP, IKK16, TPCA1, and Amlexanox) as controls; the chemical structures of these compounds were shown in **Figure 4A**. The luminescent kinase assay results indicated that NDSM253 inhibited IKK1 activity with an IC₅₀=13.5±1.21 nM (**Figure 4B**). By contrast, the IC₅₀s of ACHP, IKK16, and TPCA1 for inhibition of IKK1 were 182.5±11.3 nM, 205.4±14.5 nM, and 432.1±31.1 nM, respectively (**Figure 4B**). We also determined the IC₅₀ values of NDSM253, ACHP, IKK16, and TPCA1 for the inhibition of IKK2 and obtained IC₅₀ values of 745.6±54.3 nM, 9.4±0.72 nM, 52.4±4.3 nM, and 21.5±31.9 nM, respectively (**Figure 4C**). The luminescent kinase assay results for the

evaluation of IC₅₀ values of NDSM253, ACHP, IKK16, and Amlexanox indicated that the IC₅₀s of these chemicals were 81.6±7.3 mM, 87.7±7.8 mM, 73.2±6.4 mM, and 2.5±0.2 mM, respectively (**Figure 4D**). The lower IC₅₀ but higher or similar IC₅₀ of NDSM253 than the other compounds suggested that NDSM253 was a specific IKK1 inhibitor.

NDSM253 significantly suppressed LPS-induced proinflammatory cytokine expression in vitro

We determined the *in vitro* effect of NDSM253 by treating LADMAC cells with or without LPS, followed by treatment with 14 nM NDSM253, 10 nM ACHP, 55 nM IKK16, 22 nM TPCA, or 2.5 mM Amlexanox. The harvested cells were used for RT-qPCR analyses to examine the expression of the proinflammatory cyto-

NDSM253 promotes bone healing

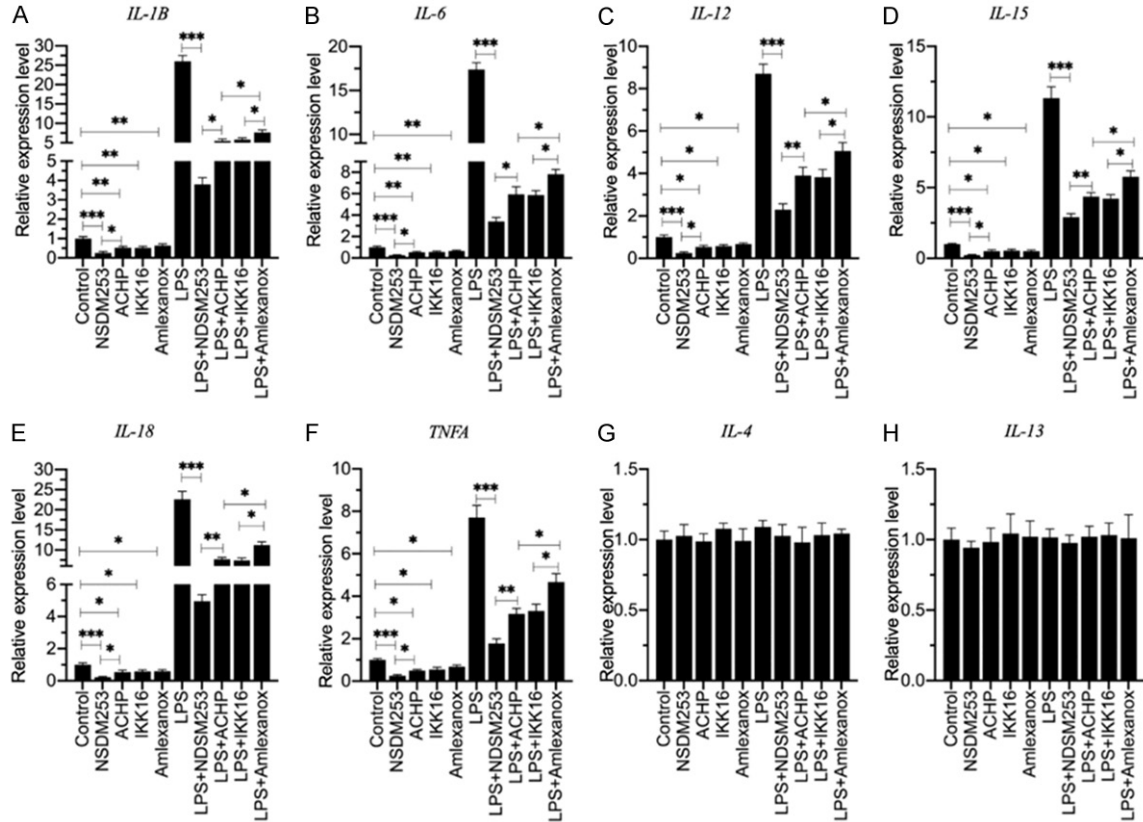


Figure 5. The effects of IKK inhibitors on the expression of proinflammatory cytokine genes *in vitro*. The LADMAC cells at 80% confluence were treated with or without 200 ng/mL LPS, followed by treatments with 14 nM NDSM253, 10 nM ACHP, 55 nM IKK16, 22 nM TPCA, and 2.5 μ M Amlexanox for 6 h. The harvested cells were subjected to RNA isolation and RT-qPCR analyses to examine the mRNA levels of *IL-1 β* (A), *IL-6* (B), *IL-12* (C), *IL-15* (D), *IL-18* (E), *TNFA* (F), *IL-4* (G), and *IL-13* (H). * P <0.05, ** P <0.01, and *** P <0.001.

kine genes *IL-1 β* (Figure 5A), *IL-6* (Figure 5B), *IL-12* (Figure 5C), *IL-15* (Figure 5D), *IL-18* (Figure 5E), and *TNFA* (Figure 5F). The expression of these six genes showed similar patterns. In both the LPS-treated or non-treated cells, NDSM253 decreased these gene expression levels most significantly, followed by ACHP, IKK16, and Amlexanox (Figure 5A-F). However, none of the four compounds significantly changed the expression of *IL-4* and *IL-13* (Figure 5G and 5H).

We examined whether this reduction also happened in the other cell lines by performing the same experiment in the macrophage-derived 23ScCr osteoclast cell line. LPS stimulation induced a significant expression of *IL-1 β* (Figure S1A), *IL-6* (Figure S1B), *IL-12* (Figure S1C), *IL-15* (Figure S1D), *IL-18* (Figure S1E), and *TNFA* (Figure S1F). NDSM253, ACHP, IKK16, and Amlexanox reduced this LPS-induced expression to different extents (Figure

S1A-F). NDSM253 caused the most significant decrease, followed by ACHP, IKK16, and Amlexanox (Figure S1A-F). None of the four compounds changed the expression of *IL-4* and *IL-13* (Figure S1G and S1H). NDSM253 therefore appeared effective for suppression of the expression of proinflammatory cytokine genes *in vitro*.

NDSM253 significantly suppressed IKK1 downstream signaling *in vitro*

We further examined how NDSM253 suppressed the expression of proinflammatory cytokine gene expression by examining the protein levels of TLR4/NF- κ B signaling molecules in the cells shown in Figure 5. The immunoblot results indicated a significant induction of TLR4, TIRAP, MyD88, TRAF6, TAK1, IKK1, and pIkB following LPS stimulation (Figure 6A and 6C). However, treatment with NDSM253, ACHP, IKK16, or Amlexanox did not change the pro-

NDSM253 promotes bone healing

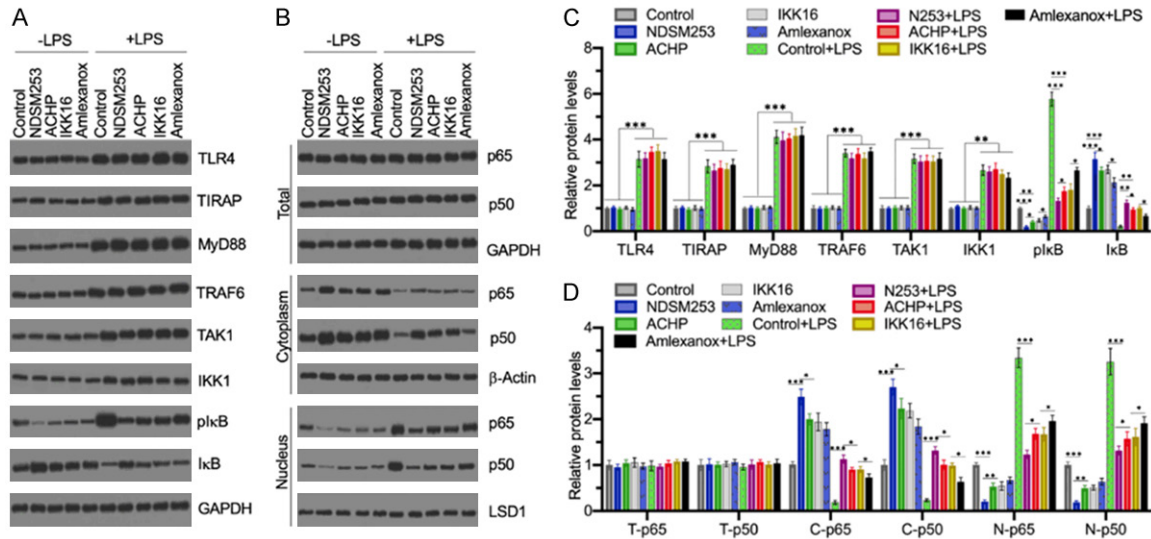


Figure 6. The *in vitro* effects of IKK inhibitors on the molecules of the TLR4/NF- κ B signaling pathway. (A) The protein levels of TLR4/NF- κ B molecules. Cells used in **Figure 5** were subjected to isolate total proteins, followed by examining the protein levels of TLR4, TIRAP, MyD88, TRAF6, TAK1, IKK1, IKK16, and I κ B by western blotting analyses. GAPDH was used as the loading control in the total cell extracts. (B) The protein levels of p65 and p50. The protein levels of p65 and p50 in the total, cytoplasmic, and nuclear portions from cells used in **Figure 5** were determined by western blotting analyses. β -Actin was used as a cytoplasmic loading control and LSD1 was used as a nuclear loading control. (C and D) The quantified protein levels. The protein bands in (A) and (B) were quantified using the Image J software and then normalized to their corresponding loading controls. (C) The quantified protein levels of (A). (D) The quantified protein levels of (B). * $P < 0.05$, ** $P < 0.01$, and *** $P < 0.001$.

tein levels of TLR4, TIRAP, MyD88, TRAF6, TAK1, or IKK1 in LPS-treated and non-treated cells (**Figure 6A** and **6C**). By contrast, I κ B phosphorylation was decreased by treatment with the IKK inhibitors (**Figure 6A** and **6C**). NDSM253 showed the most significant inhibition, followed by ACHP, IKK16, and Amlexanox (**Figure 6A** and **6C**). These IKK inhibitors showed opposite effects on the protein levels of I κ B (**Figure 6A** and **6C**), which showed accumulation in response to the IKK inhibitors (**Figure 6A** and **6C**). Neither LPS nor IKK inhibitors changed the protein levels of p65 and p50 in the total cell extracts (**Figure 6B** and **6D**).

We also isolated the cytoplasmic and nuclear fractions in the LPS- and IKK inhibitor-treated cells and determined the distributions of p65 and p50 in these two fractions. The western blotting results showed a significant decrease in the cytoplasmic fractions of p65 and p50 following LPS treatment, while IKK inhibitor treatment reversed this reduction (**Figure 6B** and **6D**). By contrast, the nuclear fractions of p65 and p50 were significantly enriched following LPS treatment, and IKK inhibitors could reverse this induction (**Figure 6B** and **6D**).

Comparison of the different effects of IKK inhibitors on changes in p65 and p50 distributions in the cytoplasm and nucleus revealed that NDSM253 had a significantly stronger effect when compared to the other three inhibitors (**Figure 6B** and **6D**). The mechanism driving the changes in proinflammatory cytokine gene expression in response to IKK inhibitor treatments therefore apparently involved inhibition of IKK1 activity and changes in the phosphorylation status of I κ B.

NDSM253 significantly decreased the serum concentration of proinflammatory cytokines in a mouse fracture model

The promising *in vitro* effects of NDSM253 on repression of LPS-induced proinflammatory cytokines encouraged us to investigate its *in vivo* effects in a mouse fracture model. After stabilizing the fractured mice, we injected IKK inhibitors every day for 10 days (**Figure 7A**). The ELISA results showed that the administration of IKK1 inhibitors significantly decreased the serum concentration of the proinflammatory cytokines IL-1 β (**Figure 7B**), IL-6 (**Figure 7C**), IL15 (**Figure 7D**), IL-18 (**Figure 7E**), and TNF- α

NDSM253 promotes bone healing

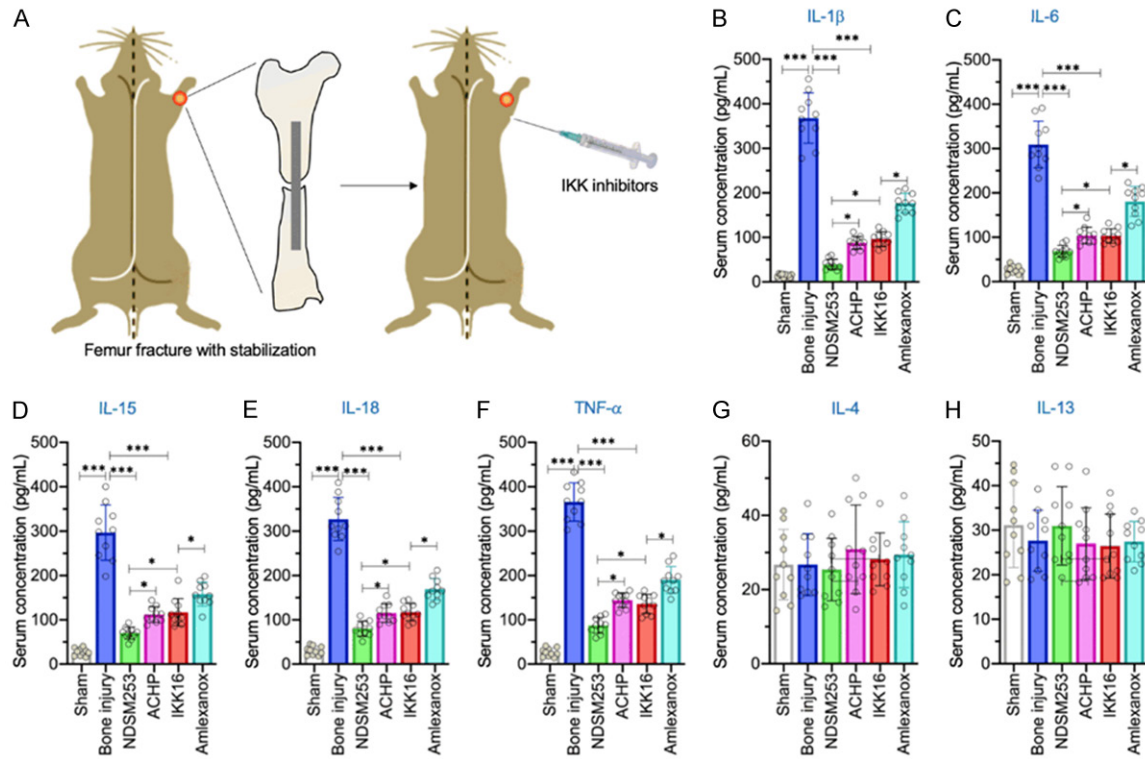


Figure 7. IKK inhibitors decreased the serum concentrations of proinflammatory cytokines *in vivo*. (A) A schematic diagram of injecting IKK inhibitors in the mouse femoral fracture model. (B-H) Serum concentrations of cytokines. Circulating levels of IL-1 β (B), IL-6 (C), IL-15 (D), IL-18 (E), TNF- α (F), IL-4 (G), and IL-13 (H) were measured in serum samples obtained from sham, bone injury, bone injury + NDSM253, bone injury + ACHP, bone injury + IKK16, and bone injury + Amlexanox group mice (n=10 for each group). *P<0.05, and ***P<0.001.

(Figure 7F). Among the IKK inhibitors, NDSM253 showed the strongest inhibitory effect on proinflammatory cytokine concentrations, followed by ACHP, IKK16, and Amlexanox (Figure 7B-F). However, none of these IKK inhibitors could change the serum concentrations of IL-4 and IL-13 (Figure 7G and 7H).

NDSM253 significantly suppressed in vivo IKK1 downstream signaling

We used callus tissues from the fractured mice given the IKK inhibitor injection and performed western blotting assays to examine the protein levels of TLR4/NF- κ B signaling molecules. The immunoblot results indicated that the IKK inhibitor treatments did not change the protein levels of TLR4, TIRAP, MyD88, TRAF6, TAK1, IKK1, or plkB (Figure 8A and 8C). However, they significantly decreased the protein level of plkB (Figure 8A and 8C). Of them, NDSM253 showed the most significant inhibition, followed by ACHP, IKK16, and Amlexanox (Figure 8A and 8C). By contrast, we found a significant accumulation of I κ B protein when the fractured mice were injected with IKK

inhibitors (Figure 8A and 8C). Consistent with the *in vitro* data, we also found no significant changes in the protein levels of p65 and p50 in mice injected with IKK inhibitors compared to non-injected mice (Figure 8B and 8D). We also isolated the cytoplasmic and nuclear fractions in tissues from different groups of mice and determined the distributions of p65 and p50. The IKK inhibitor treatments increased the accumulation of both p65 and p50 in the cytoplasm (Figure 8B and 8D). By contrast, the injection of IKK inhibitors decreased the protein levels of p65 and p50 in the nucleus (Figure 8B and 8D). NDSM253 showed a significantly stronger effect than the other three inhibitors (Figure 8B and 8D), suggesting that NDSM253 was also effective *in vivo* at inhibiting IKK1, thereby inhibiting proinflammatory cytokine effects.

NDSM253 significantly promoted bone healing in the fractured mice

We also examined whether the NDSM253-induced decrease in proinflammatory cytokine concentrations might play a role in bone heal-

NDSM253 promotes bone healing

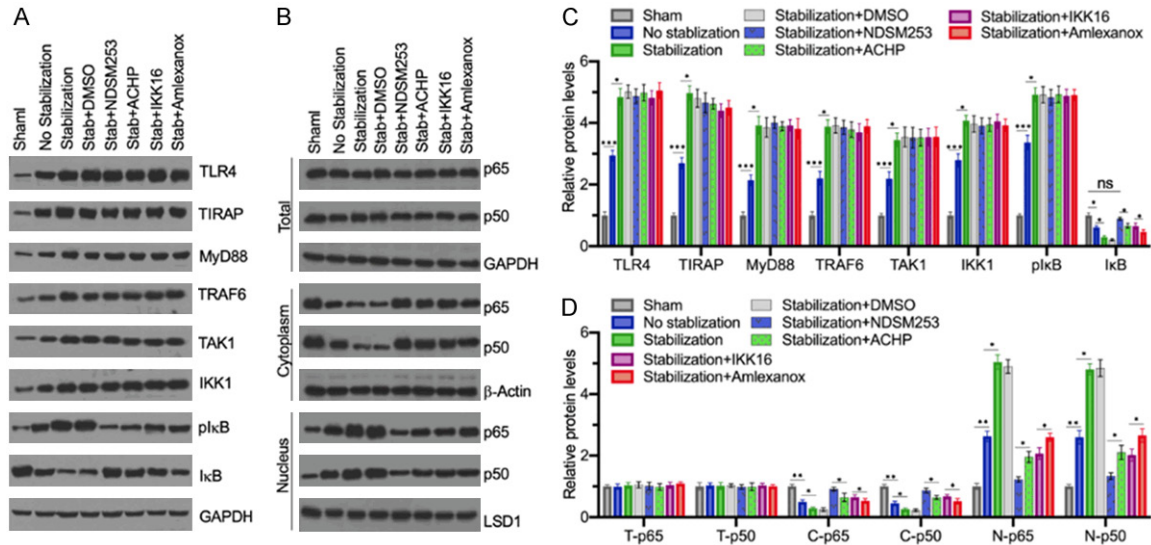


Figure 8. The effects of IKK inhibitors on the molecules of TLR4/NF- κ B signaling pathway *in vivo*. (A) The protein levels of TLR4/NF- κ B molecules. Total proteins isolated from callus around the fracture sites were used to examine the protein levels of TLR4, TIRAP, MyD88, TRAF6, TAK1, IKK1, pI κ B, and I κ B by western blotting analyses. GAPDH was used as the loading control in the total cell extracts. (B) The protein levels of p65 and p50. The protein levels of p65 and p50 in the total, cytoplasmic and nuclear portions from callus around the fracture sites were determined by western blotting analyses. β -Actin was used as a cytoplasmic loading control and LSD1 was used as a nuclear loading control. (C and D) The quantified protein levels. The protein bands in (A) and (B) were quantified using the Image J software and then normalized to their corresponding loading controls. (C) The quantified protein levels of (A). (D) The quantified protein levels of (B). * $P < 0.05$, ** $P < 0.01$, and *** $P < 0.001$.

ing. We injected IKK inhibitors daily for 30 days and then scored the callus formation and bone union in the mouse fractures (**Figure 9A**). The callus formation scores confirmed that the administration of IKK inhibitors significantly promoted the formation of callus when the mice were stabilized with stainless steel (**Figure 9B**). Similarly, the bone union score results also indicated that IKK inhibitors markedly increased the formation of a bone bridge union (**Figure 9C**). Among the IKK inhibitors, NDSM253 showed the most significant effect in promoting the formation of calluses and bone union, followed by ACHP, IKK16, and Amlexanox (**Figure 9B** and **9C**).

Discussion

The transcription of proinflammatory cytokine genes is mainly controlled by the NF- κ B transcription factor [10]. Harmful stimulation can activate TLR4 signaling, causing the translocation of NF- κ B subunits from the cytoplasm to the nucleus (**Figure 10**). Proinflammatory cytokines have been shown to play roles in different stages of bone fracture [3, 6]. Excessive amounts of proinflammatory cytokines result in

a severe inflammation response and cause tissue damage [3, 6]. Therefore, blocking the TLR4/NF- κ B signaling to suppress proinflammatory cytokines is an effective strategy for inhibiting inflammation responses [10]. In the present study, we discovered that NDSM253 could significantly block IKK downstream signaling, causing a decrease in pI κ B but an increase in I κ B, a compound that binds to NF- κ B subunits and limits their nuclear translocation (**Figure 10**). The decreased accumulation of NF- κ B subunits in the nucleus then suppresses the expression of proinflammatory cytokine genes, decreasing the inflammation response and improving bone healing (**Figure 10**).

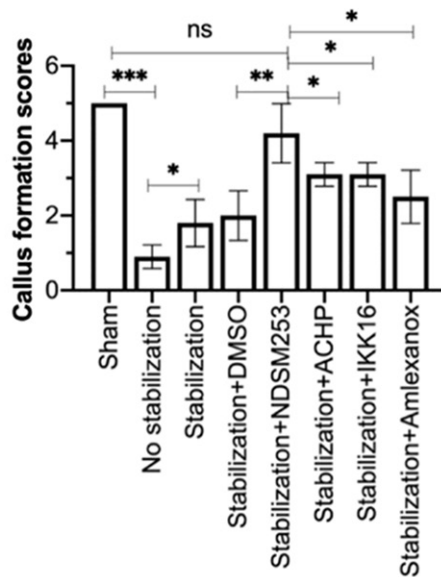
A great number of small molecules have been shown to interfere with IKKs [13-19]. However, many of them also have other targets apart from IKKs [13-19]. Small molecules with multiple targets have only limited experimental and clinical uses. In this study, we discovered that a low dose of NDSM253 (14 nM) could significantly inhibit IKK1 activity while only weakly affecting IKK2 and IKKe activities. The high specificity and inhibitory efficiency of NDSM253

A

Scoring system for fracture healing

Categories	Scores					
	5	4	3	2	1	0
Callus formation	Full-across the fracture	High (>70% across)	Moderate across (70-50%)	Moderate/mild across (25-50%)	Mild across (<25%)	None
Bone union	Full bone bridge union	High (>70% bridge)	Moderate (70-50%)	Moderate/mild (25-50%)	Mild (<25%)	None

B



C

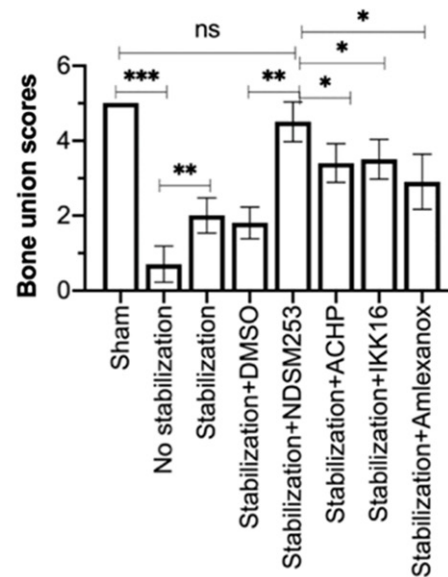


Figure 9. Administration of NDSM253 in fractured mice significantly promote bone healing. (A) The scoring system of bone healing. Two categories, including callus formation and bone union formation, were set as score standards. (B) The scores of callus formation in different groups of mice, including sham, non-stabilization, stabilization, stabilization + DMSO, stabilization + NDSM253, stabilization + ACHP, stabilization + IKK16, and stabilization + Amlexanox, were recorded. ns = no significant difference, * $P < 0.05$, ** $P < 0.01$, and *** $P < 0.001$. (C) The scores of bone union formation in the same groups of mice as (A) were recorded. ns = no significant difference, * $P < 0.05$, ** $P < 0.01$, and *** $P < 0.001$.

imply that it may be a useful IKK1 inhibitor in the future. To our knowledge, NDSM253 has not yet been determined to play a role in any biological process. A comparison of the chemical structure of NDSM253 with other IKK inhibitors does not reveal any structural similarity, suggesting that it may have a specific binding site for IKK1. In the current study, we focused on the pharmacological role of NDSM253 in inhibiting IKK1-downstream molecules. We are currently making efforts to dissolve the binding site of NDSM253 in IKK1.

The bone healing process has many barriers, and the dysregulated inflammation response is

the most important [2, 3]. However, current animal bone fracture models mainly focus on surgical techniques and bone regeneration stimulators. In our current fracture model, we evaluated the suppression of proinflammatory cytokines as a way to improve bone healing. Our results clearly showed that the inhibition of proinflammatory cytokines could significantly promote bone healing, implicating this as a potential new therapeutic strategy for bone fracture treatment in the future. The activation of TLR4/NF- κ B signaling is a common phenomenon in inflammation diseases [10]. Although we only examined the *in vivo* effect of NDSM253 in bone fracture, the promising *in*

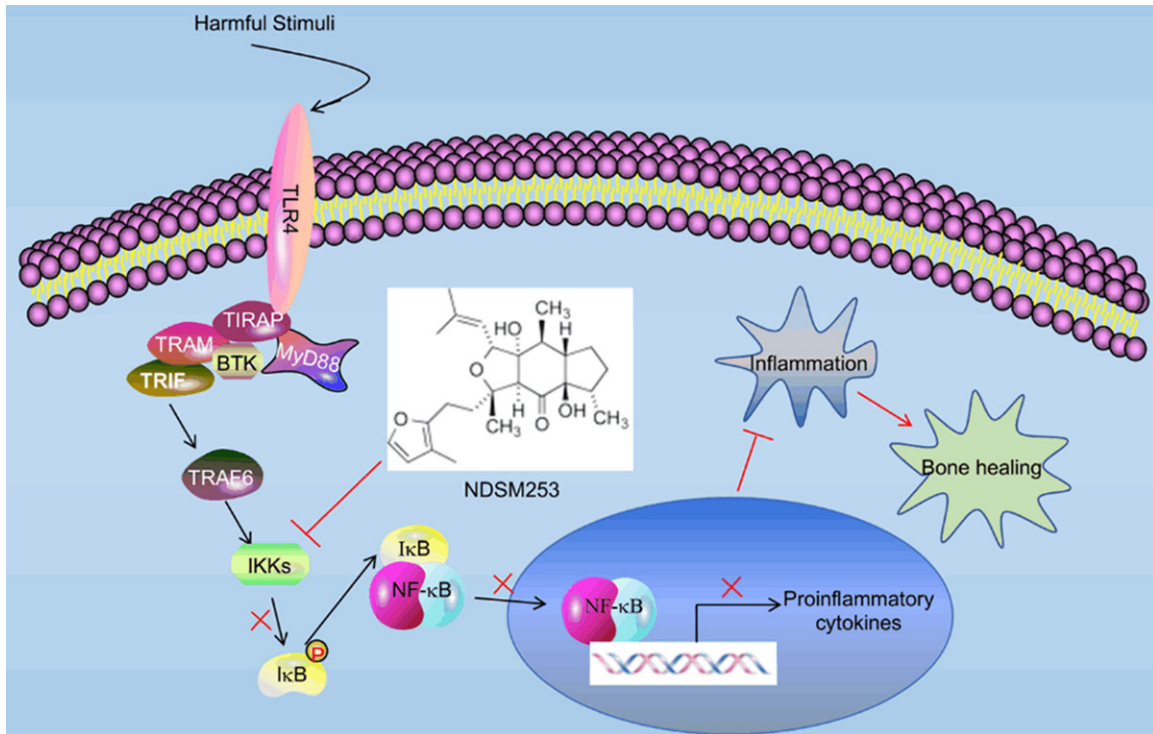


Figure 10. The schematic diagram of NDSM253 targeting IKK1 to inhibit the inflammatory response and promote fracture healing. Once a bone is injured, macrophages are recruited to the fractured sites and the TLR4/NF-κB signaling is activated, causing the induction of a kinase cascade, including TAK1 and IKK1. IKK1 phosphorylates IκB, leading to its dissociation from NF-κB. The free IκB is degraded by the proteasome. NF-κB enters into the nucleus and initiates proinflammatory cytokine gene expression, causing the inflammation response. The excessive inflammation response results in tissue damage and disrupts bone healing. NDSM253 specifically inhibits IKK1, causing the impairment of IKK-downstream signaling, limiting the nuclear translocation of NF-κB, and decreasing the expression of proinflammatory cytokines. Decreased inflammation response promotes bone healing.

in vitro results in LPS-induced macrophages strongly suggest that NDSM253 may also be effective in inhibiting the induction of proinflammatory cytokines and improving the outcomes of other inflammatory diseases.

In summary, we reveal that TLR4/NF-κB signaling and proinflammatory cytokines are activated in a mouse fracture model. Using the FLECS method, we identified an IKK1 inhibitor NDSM253 that significantly inhibited IKK1 activity and impaired IKK downstream signaling, resulting in a decrease in proinflammatory cytokine levels and a promotion of bone healing.

Acknowledgements

We thank Dr. Wantong Liang for his help to design the experiments and carefully revising the manuscript.

Disclosure of conflict of interest

None.

Address correspondence to: Lin Liu and Xuekun Pan, Department of Emergency Trauma Surgery, The First People's Hospital of Yunnan Province, Kunming, Yunnan, China. E-mail: 358741303@qq.com (LL); panxuekun0871@gmail.com (XKP)

References

- [1] Loi F, Cordova LA, Pajarinen J, Lin TH, Yao Z and Goodman SB. Inflammation, fracture and bone repair. *Bone* 2016; 86: 119-130.
- [2] Mountziaris PM and Mikos AG. Modulation of the inflammatory response for enhanced bone tissue regeneration. *Tissue Eng Part B Rev* 2008; 14: 179-186.
- [3] Morgan EF, De Giacomo A and Gerstenfeld LC. Overview of skeletal repair (fracture healing and its assessment). *Methods Mol Biol* 2014; 1130: 13-31.

NDSM253 promotes bone healing

- [4] Yang P. Editorial the role of mesenchymal stem cells in bone regeneration: underlying mechanisms and systemic regulatory factors. *Curr Stem Cell Res Ther* 2017; 12: 356.
- [5] Bragdon BC and Bahney CS. Origin of reparative stem cells in fracture healing. *Curr Osteoporos Rep* 2018; 16: 490-503.
- [6] Amarasekara DS, Yun H, Kim S, Lee N, Kim H and Rho J. Regulation of osteoclast differentiation by cytokine networks. *Immune Netw* 2018; 18: e8.
- [7] Kitaura H, Kimura K, Ishida M, Kohara H, Yoshimatsu M and Takano-Yamamoto T. Immunological reaction in TNF- α -mediated osteoclast formation and bone resorption in vitro and in vivo. *Clin Dev Immunol* 2013; 2013: 181849.
- [8] Ahmed AU, Williams BR and Hannigan GE. Transcriptional activation of inflammatory genes: mechanistic insight into selectivity and diversity. *Biomolecules* 2015; 5: 3087-3111.
- [9] Kawai T and Akira S. Signaling to NF- κ B by toll-like receptors. *Trends Mol Med* 2007; 13: 460-469.
- [10] Liu T, Zhang L, Joo D and Sun SC. NF- κ B signaling in inflammation. *Signal Transduct Target Ther* 2017; 2: 17023.
- [11] Hoesel B and Schmid JA. The complexity of NF- κ B signaling in inflammation and cancer. *Mol Cancer* 2013; 12: 86.
- [12] Israel A. The IKK complex, a central regulator of NF- κ B activation. *Cold Spring Harb Perspect Biol* 2010; 2: a000158.
- [13] Llona-Minguez S, Baiget J and Mackay SP. Small-molecule inhibitors of I κ B kinase (IKK) and IKK-related kinases. *Pharm Pat Anal* 2013; 2: 481-498.
- [14] Gilmore TD and Herscovitch M. Inhibitors of NF- κ B signaling: 785 and counting. *Oncogene* 2006; 25: 6887-6899.
- [15] Prescott JA and Cook SJ. Targeting IKK β in cancer: challenges and opportunities for the therapeutic utilization of IKK β inhibitors. *Cells* 2018; 7: 115.
- [16] Zhang J, Clark K, Lawrence T, Peggie MW and Cohen P. An unexpected twist to the activation of IKK β : TAK1 primes IKK β for activation by autophosphorylation. *Biochem J* 2014; 461: 531-537.
- [17] Burke JR, Pattoli MA, Gregor KR, Brassil PJ, MacMaster JF, McIntyre KW, Yang X, Iotzova VS, Clarke W, Strnad J, Qiu Y and Zusi FC. BMS-345541 is a highly selective inhibitor of I κ B kinase that binds at an allosteric site of the enzyme and blocks NF- κ B-dependent transcription in mice. *J Biol Chem* 2003; 278: 1450-1456.
- [18] Waelchli R, Bollbuck B, Bruns C, Buhl T, Eder J, Feifel R, Hersperger R, Janser P, Revesz L, Zerwes HG and Schlapbach A. Design and preparation of 2-benzamido-pyrimidines as inhibitors of IKK. *Bioorg Med Chem Lett* 2006; 16: 108-112.
- [19] Podolin PL, Callahan JF, Bolognese BJ, Li YH, Carlson K, Davis TG, Mellor GW, Evans C and Roshak AK. Attenuation of murine collagen-induced arthritis by a novel, potent, selective small molecule inhibitor of I κ B Kinase 2, TPCA-1 (2-[(aminocarbonyl)amino]-5-(4-fluorophenyl)-3-thiophenecarboxamide), occurs via reduction of proinflammatory cytokines and antigen-induced T cell proliferation. *J Pharmacol Exp Ther* 2005; 312: 373-381.
- [20] Williams JN, Li Y, Valiya Kambrath A and Sankar U. The generation of closed femoral fractures in mice: a model to study bone healing. *J Vis Exp* 2018; 138: 58122.
- [21] Shen L, Xiao Y, Wu Q, Liu L, Zhang C and Pan X. TLR4/NF- κ B axis signaling pathway-dependent up-regulation of miR-625-5p contributes to human intervertebral disc degeneration by targeting COL1A1. *Am J Transl Res* 2019; 11: 1374-1388.
- [22] Haystead TAJ. Fluorescent-linked enzyme chemoproteomic strategy (FLECS) for identifying HSP70 inhibitors. *Methods Mol Biol* 2018; 1709: 75-86.
- [23] Sarban S, Senkoylu A, Isikan UE, Korkusuz P and Korkusuz F. Can rhBMP-2 containing collagen sponges enhance bone repair in ovariectomized rats?: a preliminary study. *Clin Orthop Relat Res* 2009; 467: 3113-3120.

NDSM253 promotes bone healing

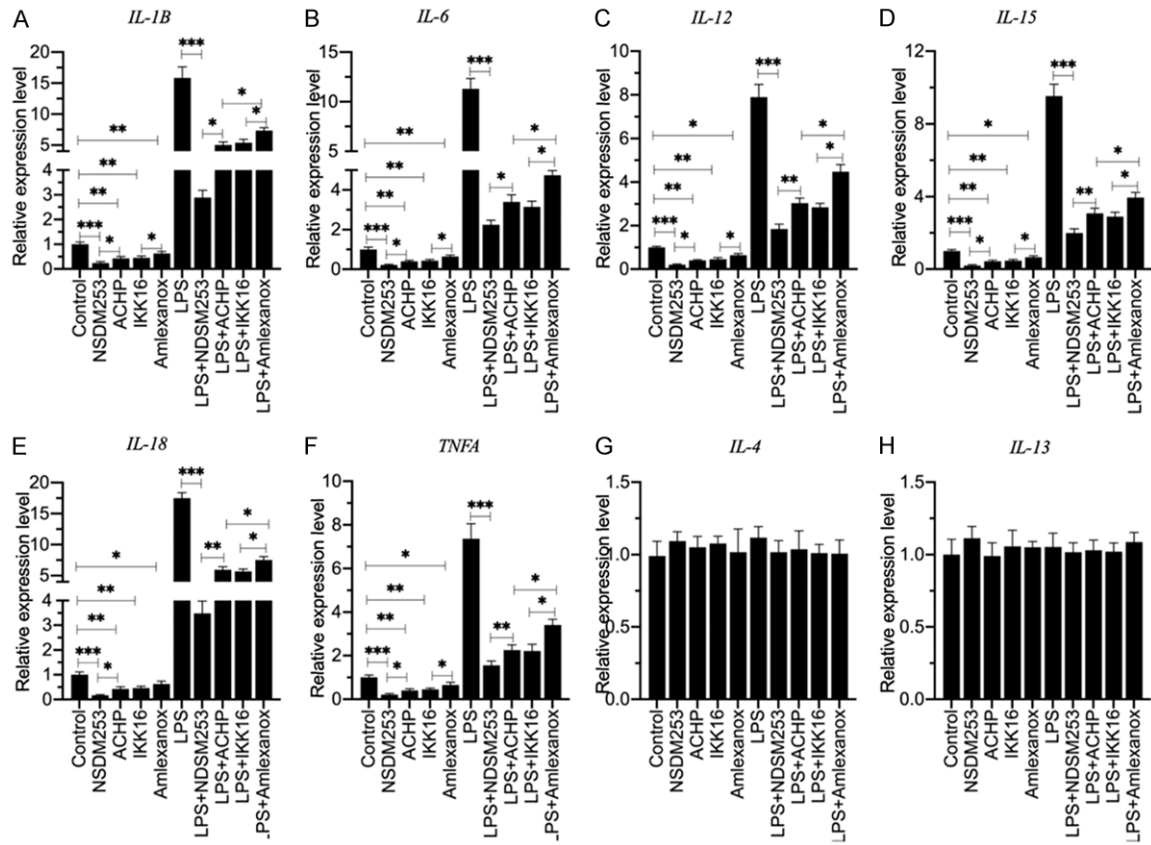


Figure S1. The effects of IKK inhibitors on the expression of proinflammatory cytokine genes in 23ScCr cells. The 23ScCr cells under 80% confluence were treated with or without 200 ng/mL LPS, followed by treatments with 14 nM NDSM253, 10 nM ACHP, 55 nM IKK16, 22 nM TPCA, and 2.5 μM Amlexanox for 6 h, respectively. The harvested cells were subjected to RNA isolation and RT-qPCR analyses to examine the mRNA levels of *IL-1β* (A), *IL-6* (B), *IL-12* (C), *IL-15* (D), *IL-18* (E), *TNFA* (F), *IL-4* (G), and *IL-13* (H). **P*<0.05, ***P*<0.01, ****P*<0.001.